

New High Heat Load Beamline Components for the ESRF

P. Marion, Y. Dabin, P. Theveneau, L. Zhang

European Synchrotron Radiation Facility, 6 rue Jules Horowitz, BP220, 38043 Grenoble Cedex, FRANCE

Phone: +33 4 7688 2032; Fax: +33 4 7688 2585

E-mail: marion@esrf.fr

Abstract

At the ESRF, the installation of small gap undulators (in vacuum undulators, small gap in air undulators) has drastically increased the beam power density delivered to the beamlines: In the last four years, the maximum power density at 27 m from the source has been increased from 230 W/mm² to 400 W/mm² and could reach 720 W/mm² in the future.

This paper describes development works carried out on some beamlines components in order to face this increased power:

- New high power (HP) primary slits have been designed, manufactured and tested. The main characteristics of the HP slits are: Beam size: 0 to 4 mm; Accuracy: 12 μ m; Repeatability: 2 μ m; Power density: 360 W/mm²; Total length: 740 mm.
- New HP attenuators are being developed. The purpose of the attenuators is to absorb the low energy photons, in order to reduce the heat load on the optical components. The HP attenuators use CVD diamond, coated with gold, as a filtering element, which should enable to absorb 70 W/mm² without thermal problem.
- Beryllium window temperature and stress predictions: When submitted to such intense beams the Be window would reach 150°C and 313 MPa. The maximum thermal stress acceptable in Be needs further investigation.

Keywords: high heat load, primary slits, attenuators, beryllium windows

1. Introduction

Third generation synchrotron light sources generate small and intense photon beams, of typically a few mm cross section and several 100 W/mm². At the ESRF, small gap undulators have been developed and installed, which generate a significantly increased photon beam power density. Table 1 gives figures for typical small gap “conventional” undulators (magnets in air, minimum gap = 11 mm) and for “in vacuum” undulators (magnets in vacuum, minimum gap = 6 mm) [1,2]. This shows that the maximum power density has been increased by a factor 2 between 1998 and 2003, and could be further increased by another factor 1.6 in the future.

In order to cope with this power increase, a new generation of front end absorbers was developed in 1999-2000. The front end components are installed on the photon beam path, at distances between 10 and 25 m from the undulator source, and are intended to collimate the beam before the beamline. The HP front end components developed, like horizontal and vertical collimators, beam shutter, and CVD diamond window are described in [3]. Several of these HP front ends have now been installed. They can accept a power density of 400 kW/mrad², and collimate the beam to 2.4 mm \times 4.8 mm (horizontal \times vertical dimension at the entrance of the beamline).

At 26 m from the undulator source, begins the beamline, in which the high heat load causes critical problems on the following components: primary slits, attenuators, windows, x-ray mirrors, and monochromators.

New developments concerning HP Primary slits, HP attenuators, and an analysis concerning beryllium windows, are detailed in the following paragraphs.

Table 1: Power Density Delivered by Typical ESRF Undulators

<i>Year</i>	<i>Undulator Type</i>	<i>Undulator Length (m)</i>	<i>Undulator Gap (mm)</i>	<i>e-beam Current (mA)</i>	<i>Max Power Density (kW/mrad²)</i>	<i>Max Power Density at 27 m from Source (W/mm²)</i>
1998	“conventional” 3 × U42	4.9	16	200	168	230
2002	“In vacuum” 1 × U33	2	6	200	175	240
2002	“conventional” 3 × U32	4.9	11	200	277	380
2003	“In vacuum” 2 × U23	4	6.8	200	335	450
Future	“In vacuum” 2 × U23	4	6	300	525	720

2. High Power Primary Slits

2.1 Old ESRF Standard Primary Slits

Before deciding to design the new HP primary slits, some investigations concerning the old ESRF standard primary slits were carried out. These slits have been installed on more than 20 of the 27 ESRF undulator beamlines, and it was necessary to analyze their behavior when submitted to the power delivered by the new generation of small gap undulators. The critical part of these slits is their horizontal blade, which is made of a water cooled Glidcop blade, inclined at 11° with respect to the incident beam.

Finite element calculations of this blade have been carried out, assuming a $2.4 \times 4.8 \text{ mm}^2$ beam, with a maximum power density of 360 W/mm^2 (this corresponds to the 450 W/mm^2 of $2 \times \text{U23}$ undulator at 200 Ma--see Table 1--from which the power absorbed by the front end diamond window has been subtracted). The results of these calculations are:

- Maximum temperatures: 750°C (surface) / 290°C (cooling channels)
- Maximum stress: 372 MPa (Von Mises)

These temperatures are considered too high for a safe operation. Some destructive tests on one blade are planned at the end of 2002 to check experimentally up to what point these slits can be used on the beamlines in safe conditions.

2.2 Specification for the HP Primary Slits

- Beam size = 0 to 4 mm Offset = +/- 5 mm maximum
- Accuracy = 15 μm Repeatability = 2 μm
- Acceptable power density > 360 W/mm²
- Total length < 760 mm (the HP slits length must not exceed the length of the old standard HP slits in order to allow easy replacement)

2.3 Principle of the HP Primary Slits

Enquiries concerning slits with similar specifications were made towards industrial companies and synchrotron laboratories. Particularly interesting ideas have been collected from slits developed at Spring-8 [4] and at APS [5-9]. Finally, it was decided to develop new slits, based on the principle of the L5-90 slits developed at APS.

Principle (see Fig. 1):

Two water-cooled masks are provided with an inner square aperture 4.3×4.3 mm inside each. Each block can be moved in Y and Z by external translation stages. The overlap between the two apertures defines a beam of variable dimensions. The stroke of the Y and Z translation stages is 12 mm.

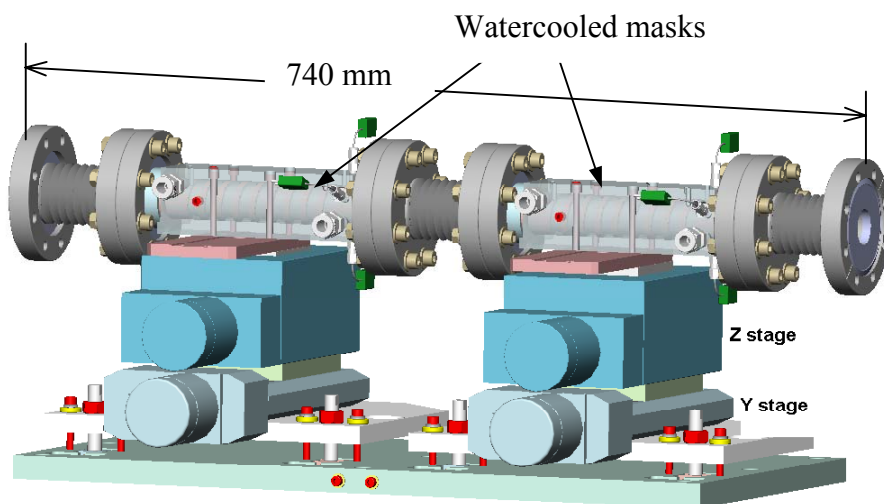


Fig. 1: Principle of the HP primary slits.

This design offers several advantages: the assembly is relatively simple and compact; it is well adapted for small and intense beams; the translation stages are located outside vacuum, completely dissociated from the slits blade, which enables commercially available translation stages to be used, provided their stiffness and angular error is sufficient.

2.4 Detailed Design of the Cooled Masks

Figure 2 shows the detailed design of the cooled masks. The main absorber (1) is made of Glidcop. Its inner surface is cut by wire erosion with a conical shape of square cross section, which ends up by a square $4.5 \text{ mm} \times 4.5 \text{ mm}$, with radii of 0.3 mm in the corners, required to reduce the stress concentrations in the corners. The incident angle with respect to the beam is 1.8° , which enables the beam to be spread over a large area. A helical channel (2) is shaped on the outside of the Glidcop main part. The dimensions of the helical channel are $10 \text{ mm} \times 3 \text{ mm}$ which provides a large water cooled area and enables the water to circulate at 5.5 m/s with no noticeable vibrations (flow rate: 10 l/mn ; measured head loss: 1.7 bar per mask ; calculated heat transfer coefficient: $19000 \text{ W.m}^{-2} \text{ } ^\circ\text{C}^{-1}$). At both ends, the Glidcop absorber is connected to NW63CF flanges via stainless steel intermediate tubular parts, sealed by vacuum brazing and TIG welding.

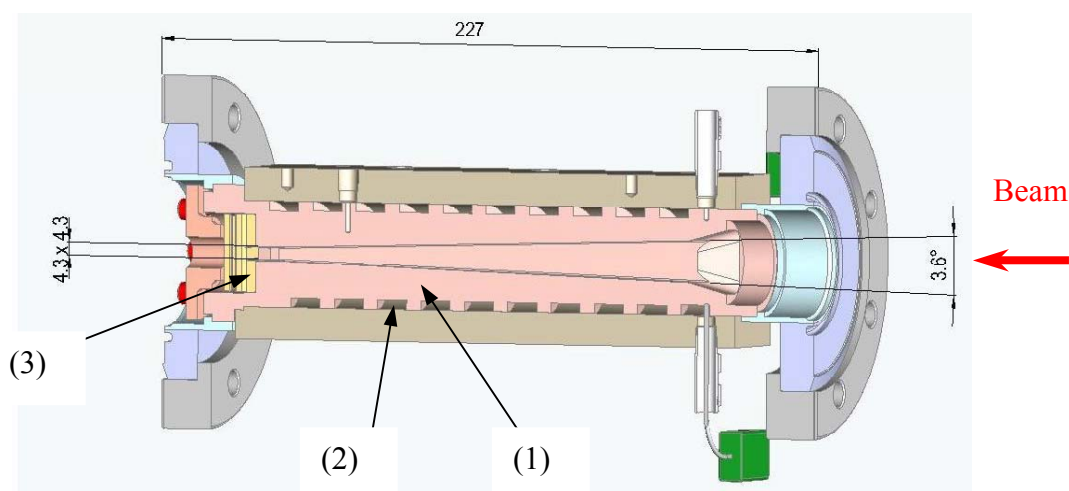


Fig. 2: HP slits - Detailed design of the cooled masks.

At the exit of the main Glidcop absorber, a diaphragm (3), provided with a perfectly square aperture of dimensions $4.3 \text{ mm} \times 4.3 \text{ mm}$, ensures the fine collimation of the beam. Its main function is to obtain a perfectly rectangular beam, in spite of the 0.3 mm radii existing in the Glidcop part. This diaphragm (3) is made of tungsten carbide with sub-micron grains, which affords an extremely high compressive strength, coupled with a reasonable heat conductivity ($70 \text{ W. m}^{-1} \text{ } ^\circ\text{K}^{-1}$), a low thermal expansion ($5.10^{-6} \text{ } ^\circ\text{K}^{-1}$) and high photon absorption. The shape of the aperture has been optimized to completely avoid the stress concentration in the corners, and to reduce the thermal stresses: the square aperture is generated by two intersecting grooves, cut by wire erosion, and the faces receiving the beam are tapered at 7° . The diaphragm (3) is clamped on part (2) with a strong contact pressure, in order to get a good thermal contact.

2.5 FEA Results

Extensive finite element analysis was carried out to assess the temperature and the stress on the parts. Some local calculations with fine mesh were done to calculate the

stress in the corners of the aperture of the Glidcop part and optimize the radii in these corners.

For a 2.4 mm × 4.8 mm beam with a maximum power density of 360 W/mm² and a Gaussian profile, the results are:

Main absorber (Glidcop):

Max. temperature = 140°C

Max. Von Mises stress = 370 Mpa

Tungsten carbide diaphragm :

Max. temperature = 600°C

Max. Von Mises stress = 370 Mpa

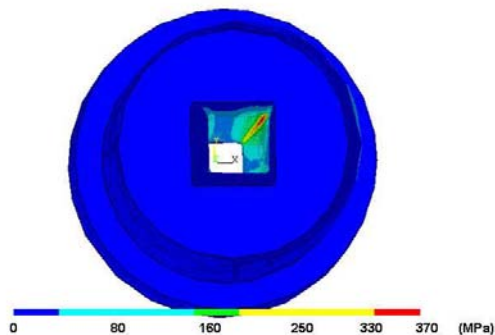


Fig. 3: HP slits - Stress map in the Glidcop absorber.

Conclusion of FEA Results :

The Glidcop temperature is low. The thermal stress in the Glidcop is higher than 200 MPa only on a very small volume (see Fig. 3). The stress level is much lower than the criterion recently proposed by L. Zhang et al. [10]. Temperatures and stresses calculated in the tungsten carbide are acceptable for this material.

2.6 Translation Tables, Accuracy Measured

An enquiry concerning commercially available Y and Z translation tables with the required specification was carried out. In order to guarantee the required precision of positioning of the slits blades, the angular error and the stiffness of the translation stages are of critical importance, in order to reduce the Abbe error and the displacement induced by the bellows forces. Typical values required are:

angular error < 70 µrad along the travel
linear stiffness better than 0.07 µm/N
angular stiffness better than 3 µrad/N.m

For the first three HP slits constructed, it was decided to use commercially available translation tables from Schneeberger (Schneeberger AG – St. Urbanstrasse 12 – Roggwil – CH – 4914 – Switzerland), which were modified to reach the specifications.

The precision of positioning was measured on the complete HP slits assembly. The displacement of each block was measured at the level of its beam defining aperture. The error on the beam aperture and offset was then calculated by cumulating the errors on each of the 2 blocks. The results are:

Error on the aperture $< 12 \mu\text{m}$

Repeatability better than $2 \mu\text{m}$

2.7 HP Slits Installed, Next Steps

Three HP slits have been installed on the ESRF beamlines ID22 and ID31 in the beginning of 2002. The operation of these slits gives full satisfaction. The HP slits have been tested up to 200 W/mm^2 on these beamlines.

Five other HP slits are being manufactured and will be installed beginning 2003.

Tests at full power on a dedicated beamline are planned in the first half of 2003.

3. High Power Attenuators

The function of the attenuators is to remove from the low energy part of the undulator spectrum from the photon beam. This enables a reduction of the heat load on the next optical components and a rejection of unwanted harmonics. This is usually achieved by placing a thin foil on the beam path. In the case of high heat load beams, it becomes impossible to absorb a significant percentage of the power using thin metallic foils without reaching excessive temperatures. This is due to the fact that the foil needs to be very thin (less than $500 \mu\text{m}$ in most cases), which does not allow the heat to be properly evacuated to the cooled border of the foil.

It has therefore been decided to develop new HP attenuators for the ESRF beamlines.

3.1 Principle of the HP Attenuators

The idea is to use a diamond CVD plate, thickness $500 \mu\text{m}$, coated with thin metallic films. Most of the power is absorbed in the thin metallic films. This power is evacuated by conduction in the diamond CVD plate, which is used as a heat sink. The temperature and thermal stress in the diamond are low, thanks to the extremely advantageous properties of the CVD diamond:

- Thermal conductivity $\approx 1900 \text{ W.m}^{-1}.\text{K}^{-1}$ (i.e., 5 times as good as copper)
- Thermal expansion $= 1 \text{ to } 4.10^{-6} \text{ }^\circ\text{K}^{-1}$ (from 300 to 700°K)
- Low photon absorption cross section, which enables to use thick plates (the thickness is in fact limited by the cost of thick CVD diamond plates)

3.2 Mechanical Design of the HP Attenuators

As can be seen in Fig. 4, the CVD diamond plate is clamped in its holder via elastic washers, which provide a 10 bar contact pressure. This can be settled carefully before installing the plate holder on the water cooled part. The water cooled part can be easily integrated in the existing ESRF attenuator mechanisms, which are installed on the beamlines.

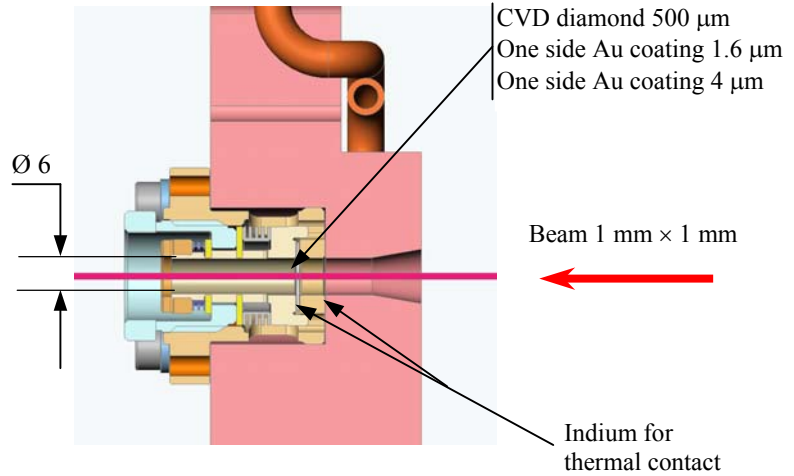


Fig. 4: HP attenuators – mechanical design.

3.3 Absorbed Power

The values of the absorbed powers in the case of a photon beam generated by an undulator 1 × U23 – gap 6 mm @ 200 mA – beamsize: 1 × 1 mm² at 28.3 m are given in Fig. 5. The total absorbed power in the HP attenuator is 69 W i.e., 33% of the incident power. It is also possible to add a standard attenuator (thin metallic foil) downstream the HP attenuator, if additional filtering is required; this additional filter will be “protected” by the HP attenuator.

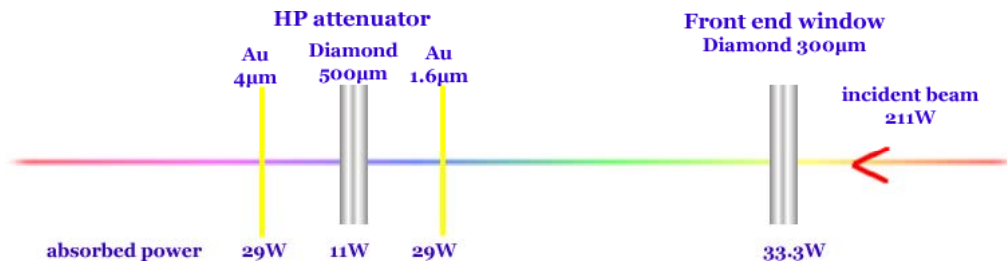


Fig. 5: Distribution of the absorbed power in the HP attenuator.

3.4 Energy Distribution

The energy distribution of the undulator beam (1 × U23 – gap 6 mm @ 200 mA) before and after the HP attenuator is shown in Fig. 6. This filtering was designed for a beamline which carries out experiments at energies higher than 30 keV.

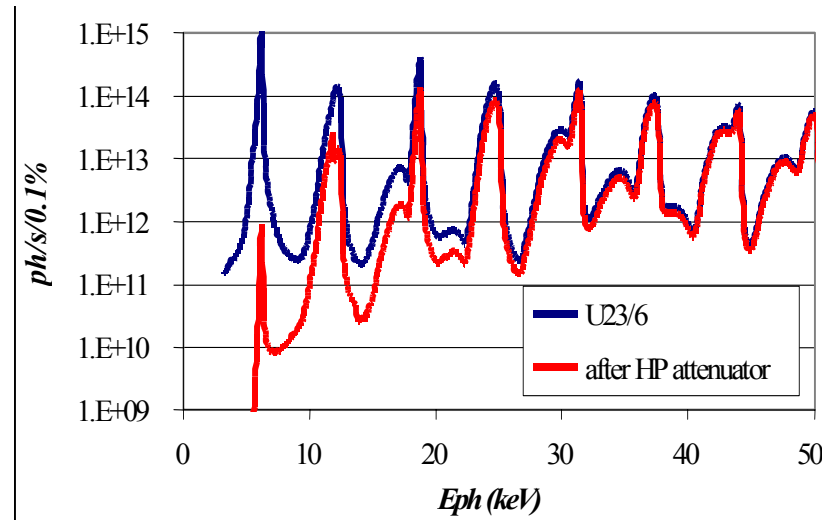


Fig. 6: Energy distribution with / without the HP attenuator.

4. Beryllium Window Temperature and Stress Predictions

Beryllium windows are often used in beamlines to insulate the vacuum of two adjacent sections. They are made of a Be foil brazed inside a water cooled copper block (see Fig. 7). The calculations presented in this paragraph give temperature and stress predictions for such windows exposed to small gap undulators beam.

4.1 Assumptions

- Window studied:
 - Beryllium window brazed in a water cooled copper block.
 - Be thickness = 0.5 mm;
Dimensions of the Be free surface = 8 mm × 20 mm
- Power source:
 - 3 × U32 undulator – gap 11 mm – 200 mA (corresponds to the 3rd line of Table 1)
 - Beam size = 2.4 × 4.8 mm (horizontal × vertical)(the beam has been collimated upstream)
 - Upstream window:

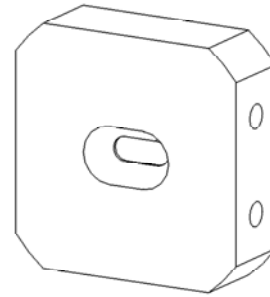
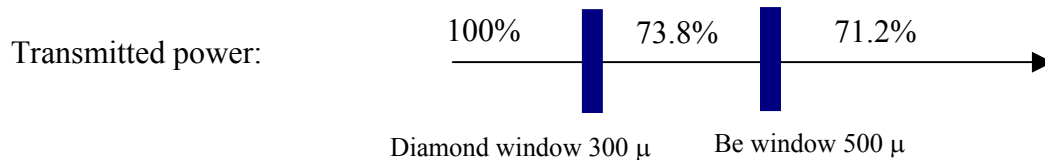


Fig. 7: Be window assembly.

Part of the power is absorbed in the diamond window (thickness 0.3 mm) located in the front end. This reduces the power absorbed in the beamline Be window.

4.2 Absorbed Power in the Window



Power absorbed in the Be window = 64 watt; Power density = 7 W/mm² max

4.3 Calculated Temperatures and Stresses in the Be Window

Stress and temperature maps are shown in Fig. 8.

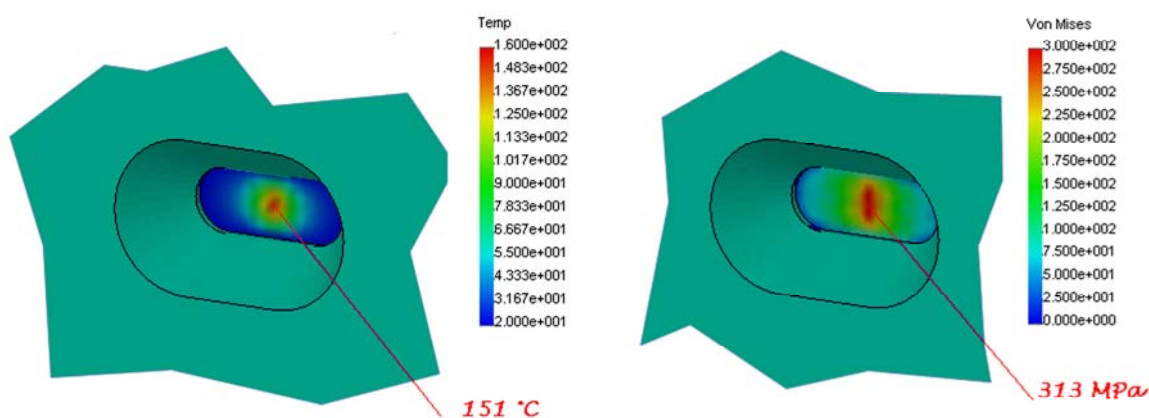


Fig. 8: Temperature and stress calculated in the beryllium window.

4.3 Conclusions

- Von Mises stresses are close to the yield tensile strength of Be (400 MPa). The safety coefficient is not large enough.
- In such cases, the Be window will be removed. An alternative solution is to replace it by a CVD diamond window developed for the ESRF front ends [3].
- A deeper study of the acceptable thermal stress in the beryllium would be useful.

5. Acknowledgments

The authors thank J. T. Collins (APS), P. Den Hartog (APS), and D. Shu (APS), for the helpful and complete information they supplied concerning the APS slits, L. Petit (ESRF) for his contribution to the hydraulic design of the HP slits, M. Nicola and H. P. Van der Kleij (ESRF) who measured the accuracy of the HP slits, and G. Retout (ESRF) for his precious help in the assembling the HP slits.

6. References

- [1] J. Chavanne et al., "Recent achievements and future prospects of ID activities at the ESRF," Proc. of EPAC 2000, Vienna (2000) 2346-2348.

- [2] J. Chavanne et al., “Construction of Apple II and in vacuum undulators at the ESRF,” Proc. of PAC 2001, Chicago (2001) 2459-2461.
- [3] J.-C. Biasci, B. Plan and L. Zhang, “Design and performance of ESRF high-power undulator front-end components,” J. Synchrotron Rad. 9 (2002). 44-46.
- [4] S. Takahashi and al., “Design of a pre-slit for Spring-8 undulator beamlines,” Proc. of SRI, Himeji (1997).
- [5] J.T. Collins, “Summary of APS white beam slit designs,” private communication.
- [6] D. Shu et al., “Design of high heatload white-beam slits for wiggler/undulator beamlines at the Advanced Photon Source,” Rev. Sci. Instrum. 66 (2), Feb. 1995.
- [7] D. Shu et al., “Thermo-mechanical analysis of the white beam slits for an undulator beamline at the Advanced Photon Source,” Rev. Sci. Instrum. 66 (2), Feb. 1995.
- [8] D. Shu et al., “Precision white beam slit design for high power density x-ray undulator beamlines at the Advanced Photon Source,” Rev. Sci. Instrum. 66 (2), Feb. 1995.
- [9] H.L. Thomas et al., “Design analysis of a composite L5-20 slit for x-ray beamlines at the Advanced Photon Source,” Rev. Sci. Instrum. 67 (9), Sept. 1996.
- [10] L. Zhang et al., “ESRF Thermal absorbers: temperature, stress and material criteria,” these proceedings.